

Communication

High-Power, Narrow-Linewidth, Continuous-Wave, Thulium-Doped Fiber Laser Based on MOPA

Biao Guan ¹, Fengping Yan ^{1,*}, Wenguo Han ¹, Qi Qin ¹ , Dandan Yang ¹, Ting Li ¹, Chenhao Yu ¹, Xiangdong Wang ¹, Kazuo Kumamoto ² , and Yuping Suo ³

¹ School of Electronic and Information Engineering, Beijing Jiaotong University, Beijing 100044, China

² Department of Electronics, Information and Communication Engineering, Osaka Institute of Technology, Osaka 535-8585, Japan

³ Shanxi Provincial People's Hospital, Shanxi Medical University, Taiyuan 030012, China

* Correspondence: fpyan@bjtu.edu.cn

Abstract: A high-power, narrow-linewidth, continuous-wave, thulium-doped fiber laser (TDFL) based on a master-oscillator power-amplifier (MOPA) was experimentally demonstrated. The main oscillator (seed source) yielded 0.64 W of narrow-linewidth laser output at a central wavelength of 1940.32 nm and a 3 dB spectral bandwidth of 0.05 nm. The output narrow-linewidth laser from the main oscillator was amplified by two-stage, cladding-pumped, thulium-doped, all-fiber amplifiers. The main amplifier yielded 26 W of narrow-linewidth laser at a central wavelength of 1940.33 nm. The slope efficiency of the main amplifier was approximately 55.6%. Significant residual pumping light component in the output laser was not observed. During the amplification process, no stimulated Brillouin scattering (SBS) effect, strong amplified spontaneous emission (ASE) effect, and parasitic lasers were observed at the reverse monitoring end. Moreover, the output power was only limited by the incident pump power and the output power had a good stability in a 50 min monitoring period.

Keywords: fiber laser; high-power; narrow-linewidth laser; MOPA; all-fiber



Citation: Guan, B.; Yan, F.; Han, W.; Qin, Q.; Yang, D.; Li, T.; Yu, C.; Wang, X.; Kumamoto, K.; Suo, Y. High-Power, Narrow-Linewidth, Continuous-Wave, Thulium-Doped Fiber Laser Based on MOPA.

Photonics **2023**, *10*, 347. <https://doi.org/10.3390/photonics10040347>

Received: 16 February 2023

Revised: 2 March 2023

Accepted: 20 March 2023

Published: 23 March 2023



Copyright: © 2023 by the authors. Licensee MDPI, Basel, Switzerland. This article is an open access article distributed under the terms and conditions of the Creative Commons Attribution (CC BY) license (<https://creativecommons.org/licenses/by/4.0/>).

1. Introduction

It has been verified that the 1.6~2.1 μm band is the output spectral range of a thulium-doped fiber laser (TDFL). Lasers in this wavelength range have good application prospects in the fields of biomedicine, industrial processing, laser radar, and laser communication [1–3]. Due to its enclosed waveguide structure, high beam quality, wide laser oscillation bandwidth, low pump threshold power, and good stability, TDFL has attracted more and more attention from the international academic community [4,5]. Nowadays, the research on high-power, narrow-linewidth, all-fiber TDFLs with 2 μm bands is an active research direction in various industries. Whether it is a laser manufacturer, a laser equipment manufacturer, or an end user, they are part of a competition to increase the output power of the TDFL [6–8].

The absorption peak of Ho: YLF and most Ho-doped vanadate crystals is 1.94 μm , and the laser conversion slope efficiency is more than 50%. TDFLs operated at 1.94 μm can be used as a pump source for a Ho-doped solid laser and it has great significance in the mid-infrared band [9–12]. This TDFL is the second-stage pump source of mid-infrared wave 3~5 μm lasers. An TDFL with an output wavelength of less than 1.95 μm is a quasi-three-level system, so there is a phenomenon of base-level reabsorption, and the shorter the wavelength, the stronger the base-level reabsorption effect. It is not easy to generate a higher power laser [13–15].

Limited by the mode volume, fiber laser oscillators usually cannot obtain high-power lasers while outputting high-quality lasers [16]. To achieve high-power laser output in the 1.94 μm band, the master-oscillator power-amplifier (MOPA) structure is mainly used to

amplify the power and energy of the low-power laser seed source. Notably, the characteristics of the seed light in the time and frequency domain are retained to the greatest extent during the amplification. Additionally, the beam quality is taken into account during the amplification, and only the power and energy of the seed source is amplified. Such a structure is conducive to solving the problems of thermal management and beam quality [17–21]. Liu et al. proposed a single-mode ZBLAN fiber with average output power of 21.8 W, with a slope efficiency of 11% [14]. Yin et al. presented an all-fiber MOPA emitting high-energy pulses and obtained an output power of 6.28 W with a slope efficiency of 32.1% [22]. Note that experimental results were unable to obtain high output power and a slope efficiency of more than half. Therefore, it is significant to investigate the effect of pumping mode to further increase power and improve the slope efficiency.

In this paper, a high-power TDFL with an all-fiber MOPA structure has been proposed and demonstrated experimentally. The seed source is a self-made, 1940 nm narrow-linewidth, continuous-wave TDFL. A narrow-linewidth, continuous-wave laser output with a center wavelength of 1940.3 nm was obtained. The 3 dB spectral bandwidth was only 0.05 nm, the maximum output power was 26 W, and the slope efficiency was 55.6%. The output power could not be further improved only using the maximum pumping power. The SBS effect, parasitic laser, and strong ASE effect were not observed in the entire system. Furthermore, the effect of the pump excitation mode on the slope efficiency was investigated and demonstrated by three structures under the same seed source.

2. Experimental Setup

The absorption spectrum of thulium ions is shown in Figure 1 [23]. Thulium ions have a variety of pumping methods, and the absorption peak near 790 nm is the largest peak. At present, multimode 793 nm laser diode (LD) technology is very mature, compared with single-mode lasers; the price of the multimode laser is only one-tenth of the single-mode lasers. In this experiment, we used 105/125 μm pigtailed 793 nm laser diodes as the pump sources to achieve full fiberization. The maximum output power was 12 W.

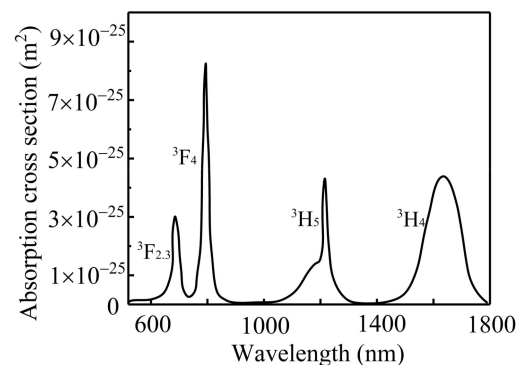


Figure 1. Absorption spectrum of thulium ions.

Figure 2 presents the experimental schematic of the proposed fiber laser. The experimental setup based on the all-fiber MOPA structure consisted of a low-power, narrow-linewidth main oscillator (seed source), and a two-stage, high-power, cladding-pumped, thulium-doped amplifier.

As shown in Figure 2a, the gain medium was a piece of 2 m double clad thulium-doped fiber (TDF, SM-TDF-10P-130M, Nufern) with a core/cladding diameter of 10/130 μm and the cladding absorption coefficient was 4.5 dB/m at 793 nm, which could provide sufficient gain for the proposed fiber laser. A pair of fiber Bragg gratings (FBGs) (with reflection ratios of 99 and 10%, respectively) were employed as the high-reflection and output ports to build the resonance cavity. Both the ports had a central wavelength of 1940 nm. The core/clad diameter for both input and output ports of FBG was 9/125 μm . The pump source was a multimode 793 nm LD and it was injected into the laser cavity through a (2 + 1) \times 1 fiber

combiner (FC). A cladding power stripper (CPS) (with a stripping efficiency of 20 dB) was spliced to the partial reflection fiber Bragg grating (PR FBG) to filter out the residual pump light, ASE, higher-order modes, and signal light leaked into the inner cladding of the fiber during splicing and bending.

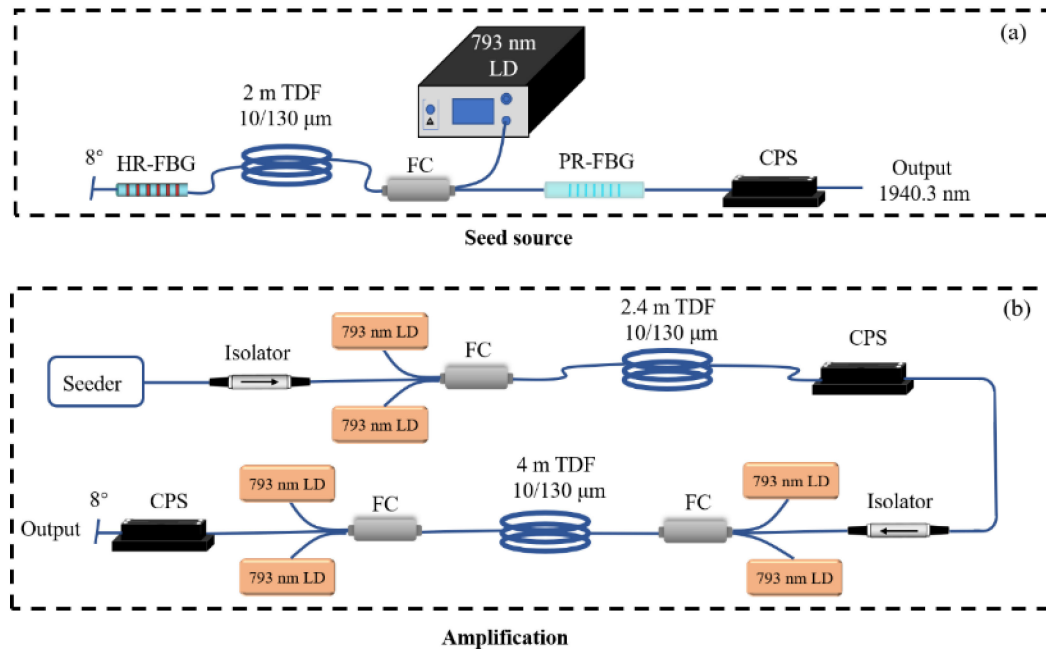


Figure 2. Schematic setup of the high-power narrow-linewidth thulium-doped all-fiber MOPA. (a) Seed source; (b) Amplification. HR: high-reflection, TDF: thulium-doped fiber, PR: partial reflection, CPS: cladding power stripper, LD: laser diode, and FC: fiber combiner.

In the pre-amplifier configuration, a 2.4 m-long double clad TDF (the same as that used in the main oscillator), two multimode 793 nm LDs, a $(2 + 1) \times 1$ fiber combiner (FC), and a CPS were employed, as shown in Figure 2b. A polarization insensitive isolator (with the maximum isolation of 48 dB and a handing power of 2 W) was located between the main oscillator and the pre-amplifier. The function of this isolator was to isolate the reflected light signal at 1940 nm and keep the temperature and power of each stage of the system as independent as possible without being affected by the previous or next stage system. The maximum output power of the total pump sources was measured to be 21.6 W after being spliced to the FCs.

The main amplifier employs a 4 m-long double clad TDF (the same as that used in the previous two stage systems), four multimode 793 nm LDs, two $(2 + 1) \times 1$ fiber combiners (FCs), and a CPS. A polarization insensitive isolator (with a maximum isolation of 30 dB and a handing power of 5 W) was located between the pre-amplifier and the main amplifier. The maximum output power of the total pump sources was measured to be 48 W after bring spliced to the FCs. The output end of the CPS was spliced with a 0.5 m-long matched passive fiber. The output end of the passive fiber was angle cleaved (8 degrees) to avoid the Fresnel reflection effect (resulting in parasitic oscillation).

Since the TDFL pumped by the 793 nm laser diodes belongs to a quasi-three-level system, the temperature of the gain medium has a great effect on the output power. Therefore, the TDF in the main amplifier was fixed on a water-cooled heat sink and maintained at a temperature of 15 °C to reduce quantum loss and improve slope efficiency. The spliced points were kept straight, and all the spliced points were coated with coating glue to avoid reflection. To obtain better laser beam quality, we reduced the coiling curvature radius of all gain fibers to ~50 mm to filter out higher-order mode lasers in the core fiber. Figure 3 shows the structures of three pumping modes.

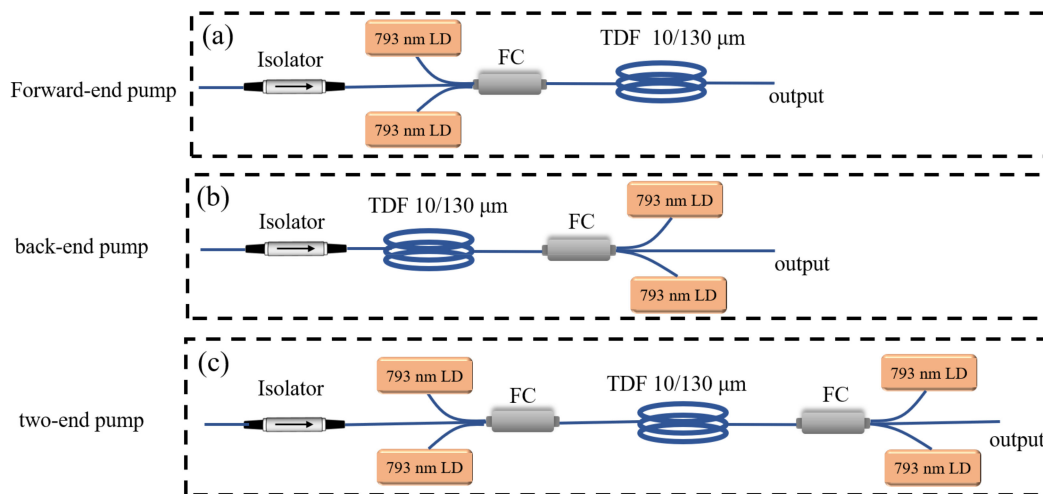


Figure 3. Schematic diagram of (a) forward-end pump, (b) back-end pump, and (c) two-end pump.

There exists a rich absorption of CO₂, H₂O, N₂O, and NH₃ in the waveband of 2 μm [24]. As the absorption of OH⁻ at 1.9 μm falls in the region, the laser source would be very useful for atmospheric LIDAR sensing, bio-medicine, and surgical applications [25–27]. Furthermore, the proposed laser realizes high power and exceptional stability with a compact structure, having potential applications in the field of material cutting, welding, and micromachining.

3. Experimental Results

Figure 4 shows the relationship between the output power of the main oscillator and the incident pump power. The pump threshold of the seed source laser was 1.4 W. The pump threshold of the seed source laser could be further reduced by reducing the loss of components. The output power of the main oscillator increased almost linearly with incident pump power. The maximum output power was 0.64 W with a slope efficiency of 14.3%.

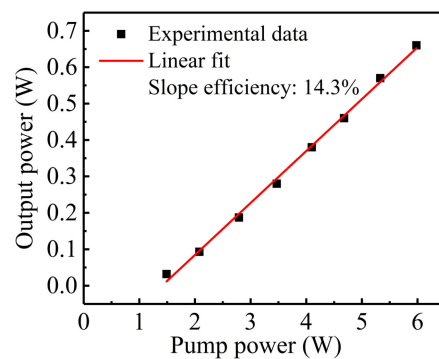


Figure 4. Output power of the main oscillator with increasing incident pump power.

The optical spectrum was measured with an optical spectrum analyzer (OSA, AQ6375 YOKOGAWA), and the result is shown in Figure 5. The center wavelength of the output laser was 1940.32 nm, which was the same as the reflection peak of FBGs. The 3 dB spectral bandwidth was 0.05 nm, and the optical signal-to-noise ratio (OSNR) was 58 dB.

In the pre-amplifier stage, when the pump power was 24 W, the pre-amplifier generated 7.8 W of output power as shown in Figure 6, and the corresponding center wavelength and spectral bandwidth were consistent with the seed source. The slope efficiency was 37.1%, corresponding to an optical efficiency of 32.5%. The TDF in the pre-amplifier stage had no cooling measures. As a result, the output power of the pre-amplifier fluctuated greatly depending on the ambient temperature.

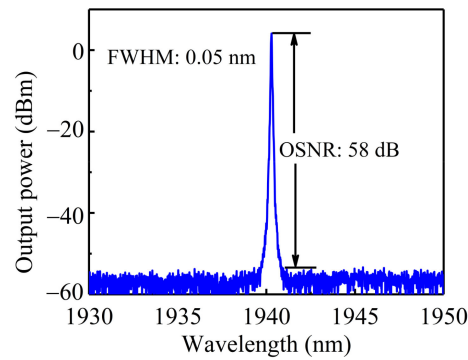


Figure 5. Optical spectrum of the thulium-doped fiber oscillator at an output power of 0.64 W.

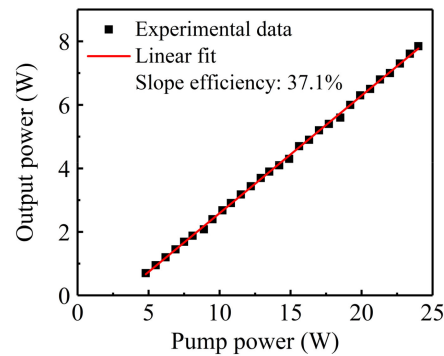


Figure 6. Output power of the pre-amplifier with increasing incident pump power.

If the output power of the seed laser was low, the ASE effect was more likely to appear during amplification. Therefore, there must be a sufficient power of seed laser injection in the two amplifier stages to guide the signal laser amplification and suppress the ASE light. Figure 7 shows the performance of the main amplifier with a pre-amplified injection power of 7.8 W. The curves in the figure indicate that gain saturation did not occur. We monitored the output power in the three cases of forward-end pumping, back-end pumping, and two-end pumping separately. The output power of the main amplifier increased almost linearly with incident pump power. The output power achieved 26 W with a maximum two-end pumping power of ~48 W and slope efficiency of 55.6%, corresponding to an optical efficiency of 54.2%. It was obvious that we could obtain higher power and slope efficiency via the back-end pumping structure when the pumping power was lower than 24 W. If only by the forward-end or back-end pumping alone, the power of the front end or back end of the gain fiber would increase rapidly within a short distance. The corresponding temperature would also rise rapidly, resulting in unbalanced power and energy within the TDF. Therefore, in this experiment, two-end pumping was a proper choice.

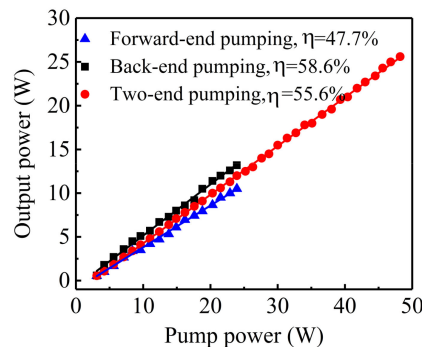


Figure 7. Output power of the main amplifier with increasing pump power.

Figure 8 shows the monitoring of the output power stability of the main amplifier. The output power was recorded using a power meter (StarLite Ophir) with a time interval of 2 min. We measured the power fluctuations of the all-fiber TDFL with an output power of 26 W. In the 50 min of running time, the output power had a fluctuation (f_p) of ± 0.4 W. This showed that the laser had good stability.

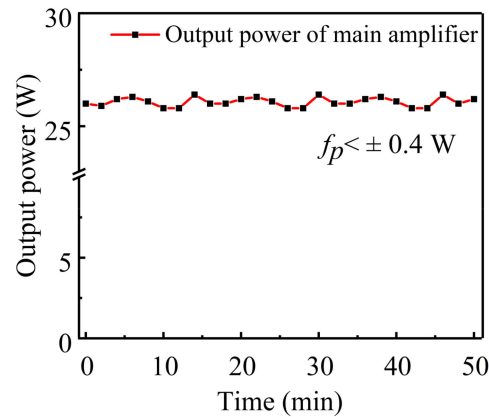


Figure 8. Output power stability of the main amplifier for 50 min.

A technical indicator comparison of our work to other proposed high power TDFLs is shown in Table 1. The comparison for the lasers was mainly at 1900~2000 nm. The maximal output power in the TDFL proposed in this paper was 26 W, which is higher than that in [14,22,28,29]. Furthermore, compared with lasers in [14,22,28–30], the slope efficiency of the proposed TDFL can reach 55.6%. The comparable and even better results observed for our laser showed the exceptional performance of our proposed TDFL.

Table 1. Technical indicator comparison of our work with other proposed high power TDFLs.

Reference	Wavelength/nm	Maximal Output Power/W	Slope Efficiency
[14]	1963	21.8	11%
[22]	1958	6.28	30.4%
[28]	2000.9	6.42	32.1%
[29]	1971.8	24.8	50.5%
[30]	1950	28	47.3%
This work	1940.33	26	55.6%

4. Conclusions

In conclusion, we proposed and demonstrated a 26 W all-fiber, narrow-linewidth, thulium-doped fiber MOPA at a central wavelength of 1940.33 nm and a 3 dB spectral bandwidth of 0.05 nm. The output power was only limited by the available pump source. During the amplification process, no SBS effect, a strong ASE effect, and parasitic lasers were observed at the reverse monitoring end. The comprehensive performance of the proposed fiber laser was satisfactory, and there is room for further improvement in single index, such as higher power, higher efficiency, narrower linewidth, etc.

Author Contributions: Conceptualization, B.G.; methodology, B.G. and F.Y.; software, D.Y. and W.H.; validation, Q.Q. and T.L.; resources, C.Y. and X.W.; data curation, D.Y. and K.K.; writing—original draft preparation, Y.S. and X.W.; writing—review and editing, B.G. and W.H.; supervision, B.G. and Q.Q.; project administration, B.G. All authors have read and agreed to the published version of the manuscript.

Funding: This research was supported by the Fundamental Research Funds for the Central Universities (No. 2022JBCG005) and National Natural Science Foundation of China (No. 61827818, 61975105).

Institutional Review Board Statement: Not applicable.

Informed Consent Statement: Not applicable.

Data Availability Statement: The data presented in this study is available from the corresponding author upon reasonable request.

Conflicts of Interest: The authors declare no conflict of interest.

References

1. Zheng, H.; Zhang, J.; Guo, N.; Zhu, T. Distributed optical fiber sensor for dynamic measurement. *J. Light. Technol.* **2021**, *39*, 3801–3811. [[CrossRef](#)]
2. Agger, S.; Povlsen, J.H.; Varming, P. Single-frequency thulium-doped distributed-feedback fiber laser. *Opt. Lett.* **2004**, *29*, 1503–1505. [[CrossRef](#)] [[PubMed](#)]
3. Henderson, S.W.; Suni, P.J.M.; Hale, C.P.; Hannon, S.M.; Magee, J.R.; Bruns, D.L.; Yuen, E.H. Coherent laser radar at 2 μm using solid-state lasers. *IEEE Trans. Geosci. Remote Sens.* **1993**, *31*, 4–15. [[CrossRef](#)]
4. Koch, G.J.; Beyon, J.Y.; Barnes, B.W.; Petros, M.; Yu, J.; Amzajerdian, F.; Kavaya, M.J.; Singh, U.N. High-energy 2 μm Doppler lidar for wind measurements. *Opt. Eng.* **2007**, *46*, 116201.
5. Liao, R.; Song, Y.; Liu, W.; Shi, H.; Chai, L.; Hu, M. Dual-comb spectroscopy with a single free-running thulium-doped fiber laser. *Opt. Express* **2018**, *26*, 11046–11054. [[CrossRef](#)]
6. Moulton, P.F.; Rines, G.A.; Slobodtchikov, E.V.; Wall, K.F.; Frith, G.; Samson, B.; Carter, A.L.G. Tm-doped fiber lasers: Fundamentals and power scaling. *IEEE J. Sel. Top. Quantum Electron.* **2009**, *15*, 85–92. [[CrossRef](#)]
7. Jackson, S.D. Towards high-power mid-infrared emission from a fibre laser. *Nat. Photonics* **2012**, *6*, 423–431. [[CrossRef](#)]
8. Geng, J.; Wang, Q.; Jiang, S. 2 μm fiber laser sources their applications. In Proceedings of the Nanophotonics Macrophotonics for Space Environments, V, San Diego, CA, USA, 21–25 August 2011; SPIE-International Society for Optical Engineering: Bellingham, WA, USA, 2011; Volume 8164, pp. 79–88.
9. Sarp, A.S.K.; Gulsoy, M. Determining the optimal dose of 1940-nm thulium fiber laser for assisting the endodontic treatment. *Lasers Med. Sci.* **2017**, *32*, 1507–1516. [[CrossRef](#)]
10. Ahmadi, P.; Estrada, A.; Katta, N.; Lim, E.; McElroy, A.; Milner, T.E.; Mogan, V.; Underwood, M. 1940 nm all-fiber Q-switched fiber laser. In Proceedings of the Fiber Lasers XIV: Technology and Systems, San Francisco, CA, USA, 28 January–2 February 2017; SPIE-International Society for Optical Engineering: Bellingham, WA, USA, 2017; Volume 10083, pp. 71–77.
11. Yang, C.; Ju, Y.L.; Yao, B.Q.; Dai, T.Y.; Duan, X.M.; Zhang, Z.G.; Liu, W. 140 W high power all-fiber laser at 1940 nm with narrow spectral line-width by MOPA configuration. *Appl. Phys. B* **2016**, *122*, 230. [[CrossRef](#)]
12. Zhang, Z.; Boyland, A.J.; Sahu, J.K.; Clarkson, W.A.; Ibsen, M. High-power single-frequency thulium-doped fiber DBR laser at 1943 nm. *IEEE Photonics Technol. Lett.* **2011**, *23*, 417–419. [[CrossRef](#)]
13. Frith, G.; Carter, A.; Samson, B.; Town, G. Design considerations for short-wavelength operation of 790-nm-pumped Tm-doped fibers. *Appl. Opt.* **2009**, *48*, 5072–5075. [[CrossRef](#)]
14. Liu, K.; Liu, J.; Shi, H.; Tan, F.; Wang, P. High power mid-infrared supercontinuum generation in a single-mode ZBLAN fiber with up to 21.8 W average output power. *Opt. Express* **2014**, *22*, 24384–24391. [[CrossRef](#)]
15. Simakov, N.; Davidson, A.; Hemming, A.; Bennetts, S.; Hughes, M.; Carmody, N.; Davies, P.; Haub, J. Mid-infrared generation in ZnGeP2 pumped by a monolithic, power scalable 2- μm source. In Proceedings of the Fiber Lasers IX: Technology, Systems, and Applications, San Francisco, CA, USA, 21–26 January 2012; SPIE-International Society for Optical Engineering: Bellingham, WA, USA, 2012; Volume 8237, pp. 559–564.
16. Liu, J.; Liu, K.; Shi, H.; Hou, Y.; Jiang, Y.; Wang, P. 210 W single-frequency, single-polarization, thulium-doped all-fiber MOPA. *Opt. Express* **2014**, *22*, 13572–13578. [[CrossRef](#)]
17. Shi, H.; Liu, J.; Liu, K.; Tan, F.; Wang, P. 160 W average power single-polarization, nanosecond pulses generation from diode-seeded thulium-doped all fiber MOPA system. In Proceedings of the Fiber Lasers XII: Technology, Systems, and Applications, San Francisco, CA, USA, 7–12 February 2015; SPIE-International Society for Optical Engineering: Bellingham, WA, USA, 2015; Volume 9344, pp. 258–263.
18. Yao, B.Q.; Li, H.; Li, X.L.; Chen, Y.; Duan, X.M.; Bai, S.; Yang, H.Y.; Cui, Z.; Shen, Y.J.; Dai, T.Y. An actively mode-locked Ho: YAG solid-laser pumped by a Tm-doped fiber laser. *Chin. Phys. Lett.* **2016**, *33*, 044205. [[CrossRef](#)]
19. Geng, J.; Wang, Q.; Luo, T.; Jiang, S.; Amzajerdian, F. Single-frequency narrow-linewidth Tm-doped fiber laser using silicate glass fiber. *Opt. Lett.* **2009**, *34*, 3493–3495. [[CrossRef](#)]
20. Hu, J.; Menyuk, C.R.; Shaw, L.B.; Sanghera, J.S.; Aggarwal, I.D. Computational study of 3–5 μm source created by using supercontinuum generation in As₂S₃ chalcogenide fibers with a pump at 2 μm . *Opt. Lett.* **2010**, *35*, 2907–2909. [[CrossRef](#)]
21. Lippert, E.; Fonnum, H.; Stenersen, K. High power multi-wavelength infrared source. In Proceedings of the Technologies for Optical Countermeasures VII, Toulouse, France, 20–23 September 2010; SPIE-International Society for Optical Engineering: Bellingham, WA, USA, 2010; Volume 7836, pp. 99–104.
22. Yin, K.; Yang, W.; Zhang, B.; Li, Y.; Hou, J. Microsecond gain-switched master oscillator power amplifier (1958 nm) with high pulse energy. *Quantum Electron.* **2014**, *44*, 163. [[CrossRef](#)] [[PubMed](#)]

23. Jackson, S.D.; King, T.A. Theoretical modeling of Tm-doped silica fiber lasers. *J. Light. Technol.* **1999**, *17*, 948. [[CrossRef](#)]
24. Mihalcea, R.M.; Webber, M.E.; Baer, D.S.; Hanson, R.K.; Feller, G.S.; Chapman, W.B. Diode-laser absorption measurements of CO₂, H₂O, N₂O, and NH₃ near 2.0 μm. *Appl. Phys. B* **1998**, *67*, 283–288. [[CrossRef](#)]
25. Shi, W.; Petersen, E.B.; Moor, N.; Chavez-Pirson, A.; Peyghambarian, N. Single frequency actively Q-switched 2 μm fiber laser by using highly Tm-doped Germanate fiber. In *CLEO: Science and Innovations*; Optica Publishing Group: Washington, DC, USA, 2011; p. CThDD6.
26. Blackmon, R.L.; Case, J.R.; Trammell, S.R.; Irby, P.B.; Fried, N.M. Fiber-optic manipulation of urinary stone phantoms using holmium: YAG and thulium fiber lasers. *J. Biomed. Opt.* **2013**, *18*, 028001. [[CrossRef](#)]
27. Wenk, S.; Furst, S.; Danicke, V.; Kunde, D.T. Design and technical concept of a Tm laser scalpel for clinical investigation based on a 60 W, 1.92 μm Tm fiber laser system. *Adv. Med. Eng. V* **2007**, *114*, 447–452.
28. Stachowiak, D.; Kaczmarek, P.; Abramski, K.M. High-power pump combiners for Tm-doped fibre lasers. *Opto-Electron. Rev.* **2015**, *23*, 259–264. [[CrossRef](#)]
29. Pei, W.; Li, H.; Cui, Y.; Zhou, Z.; Wang, M.; Wang, Z. Narrow-linewidth 2 μm all-fiber laser amplifier with a highly stable and precisely tunable wavelength for gas molecule absorption in photonic crystal hollow-core fibers. *Molecules* **2021**, *26*, 5323. [[CrossRef](#)]
30. Wang, J.; Yeom, D.; Lee, S.B.; Lee, K. 28 W CW linearly polarized single mode all-fiber thulium-doped fiber laser operating at 1.95 μm. *Opt. Eng.* **2017**, *56*, 046108. [[CrossRef](#)]

Disclaimer/Publisher’s Note: The statements, opinions and data contained in all publications are solely those of the individual author(s) and contributor(s) and not of MDPI and/or the editor(s). MDPI and/or the editor(s) disclaim responsibility for any injury to people or property resulting from any ideas, methods, instructions or products referred to in the content.